Hindawi
Complexity
Volume 2022, Article ID 2992379, 21 pages
https://doi.org/10.1155/2022/2992379

Research Article

Planning the Emergency Collision Avoidance Strategy Based on Personal Zones for Safe Human-Machine Interaction in Smart Cyber-Physical System

Thanh Phuong Nguyen,[1] Hung Nguyen,[1] and Ha Quang Thinh Ngo [2,3]

[1]*HUTECH Institute of Engineering, HUTECH University, Ho Chi Minh, Vietnam*
[2]*Department of Mechatronics, Faculty of Mechanical Engineering, Ho Chi Minh City University of Technology (HCMUT), 268 Ly Thuong Kiet Street, District 10, HCMC, 700000, Vietnam*
[3]*Vietnam National University Ho Chi Minh City, Linh Trung Ward, Thu Duc District, Ho Chi Minh, 700000, Vietnam*

Correspondence should be addressed to Ha Quang Thinh Ngo; nhqthinh@hcmut.edu.vn

Received 12 May 2021; Revised 16 February 2022; Accepted 24 February 2022; Published 30 March 2022

Academic Editor: Hang Su

Human contact is a key issue in social interactions for autonomous systems since robots are increasingly appearing everywhere, which has led to a higher risk of conflict. Particularly in the real world, collisions between humans and machines may result in catastrophic accidents or damaged goods. In this paper, a novel stop strategy related to autonomous systems is proposed. This control method can eliminate the vibrations produced by a system's movement by analysing the poles and zeros in the model of autonomous vehicles and goods. Using the pole placement technique, the motion of a system is guaranteed to be more stable, more flexible and smoother. Moreover, several control profiles are employed in the switching mechanism to choose the proper vibration-free effect. The main contributions of this paper are (i) the recommendation of an active stopping planner using different smooth generators from a modelling study, (ii) the validation of their physical characteristics and (iii) the launching of a switching algorithm based on the socially aware navigation framework of a robot. This theoretical work is based on the virtual environment of MATLAB, and the experiment is implemented in the practical platform of an automated guided vehicle. From these results, it can be seen that the proposed approach is robust, effective and feasible for applications in storehouse management, public transportation or factory manufacturing.

1. Introduction

Together with the growth of science and technology, autonomous systems have increased considerably in the context of the industrial revolution 4.0. As a result, machines have appeared in the surrounding space of humans. In the manufacturing environment, shared space is necessary for cooperation, as it enhances industrial productivity. Typically, an autonomous robot executes its tasks in the real world. Even in the absence of men, robots should attempt to avoid conflict with other objects. As a matter of fact, the autonomous machine is able to behave more intelligently in real life.

Since social consciousness has become a popular topic, human-oriented studies have attracted not only researchers but also practitioners. All kinds of transportation models are required to complete the steering function among humans. Not all of them know how to respond in the event of a crash. One of the means of public transportations in our society is the bus, which serves many passengers. An extended optimal velocity traffic flow model on two lanes that includes a bus stop and a bus deceleration area was suggested in [1]. Two new traffic states were found such that lane-changing occurred frequently, whether ahead of or behind the bus, and the stop-and-go wave would occur on both lanes instantaneously. With the growing density of vehicles, the lane-changing region around a bus varies. Considering impact due to abnormal deceleration of the current vehicle, the traditional criticality of the working conditions is hardly able

to ensure safety [2]. A new calculation method was established in the event of a sudden reaction to maintain the criticality safety distance. It matches the demands for no injuries on an expressway as well as prevents rear-end collisions. Regarding personal characteristics, the health of a driver has an effect on driving protection. The cognitive dysfunction of a patient [3] on public roads is a subject to study. They are occasionally unable to drive owing to symptoms of executive dysfunction. Each tester was equipped with wearable sensors to analyse his/her driving behaviour. It was found that there exists a difference in deceleration posture between patients and healthy adults at an intersection. This indication can guide medical treatment for individual healthcare. Normally, most transportation on a road is carried out by private cars. As the density of traffic has increased, the risk of harm to people has also increased. To indicate regions of deceleration, the individual road markers notifying drivers of the need for deceleration have been input into a PC-based simulator [4]. The interface between the computer and participants generates a three-dimensional scene presenting visual, auditory and tactile effects. A car user's psychological feelings and visual illusions are fed back to confirm the authenticity of the situation. Regarding a person's hostility, an automatic braking system has been derived with consideration of a pleasant car owner [5]. From graphical inputs, a driver's perceived risk of collision was defined to formulate the braking support system. The findings show the need to output smooth deceleration profiles uniformly with very simple calculations. The action of braking initializes at the time of judgment to reduce speed. More generally, a driver risk evaluation method leans on the analysis of recorded driving data [6]. An estimation covering the acceleration, deceleration and steering actions is observed and scored by a risk consultant. Other types of carriers have also drawn attention from investigators. The common aero vehicle slows down its speed by performing a coning motion without a velocity profile [7]. A one-order approximate model of the velocity and long range is extracted; then, the features of the coning motion target velocity and position precision are obtained by orthogonally allocating the trajectory acceleration and velocity over the load. On the prototype of a train, the construction of an air brake and its nonlinear performance are examined [8]. The deceleration control of the pneumatic brake system is compared with different PID schemes to display its feasibility and accuracy.

2. Background Works

Safety is a constant topic of interest in numerous fields. The problem of collision avoidance mainly involves two modes of transportation: two objects moving in either opposite directions or in the same direction. Currently, the methods of ensuring safety could be categorized into passive plans and active plans. In the passive schedule, one object selects a stopping stratagem with respect to the behaviours of another. This rule offers the advantages of a dynamic braking motion, conserves kinetic energy and can afford movement in a short time. However, when faced with several objects, a time delay in communication or braking could result in serious harm. The time restriction becomes stricter because the response may not occur in time. Particularly, when an object is moving in the direction opposite to that of the driver, the human body may be wounded. Active deceleration results in a higher level of protection since one decides to halt independently. If an objector person is shown to prevail in the moving space, the driving speed of the will vehicle robustly slow down. The core of the strategy is how to break the whole system to maintain the current status.

There have been several studies concentrated on the investigation and implementation of human-machine interaction safety system which are summarized in Table 1. Some reports researched the vision-based approach that issued from tracking human's direction and computing the time or distance between operator and machine [9, 30]. The sharing fenceless space where there is no physical barrier is monitored by optical sensors. The major point is that the mentioned cyber-physical system architecture could assess the collision risk on the scale of millisecond. Based on real-time evaluation of safety distance, this leads to fast response time, trigger the safety policies and ensure the coexistence of human-machine. However, the loading status must be known and the relation between response time and image processing should be tested. In some technical investigations, the actively invisible distance from operator to robot is measured by vision-based method [31], laser scanner [10], or both [32]. Most of these studies fuse data from different sources to define the relative position, configuration of upper body or pose. Similar to the distance-based or time-based method, the space separation approach relies on the classification of working space. In the manufacturing environment, the surrounding zones of any object are categorized as three levels, such green zone, yellow zone and red zone [9]. The farthest one, named as green, is quite safe and there is no need of actions. Closing to the centre, it must deliver the alerting message or warning signal to human and robot controller must reduce speed in yellow zone. In emergency area or red zone, the notifications to inform the potential collision and, stop command or moving away command would force robot in order to prevent the collision. In the same idea but in different work, authors [33] presented a real-time safety system by allowing safe human-robot interaction at very low distances. It required to leverage known robot joint angle values and precise estimation of human's position in the working area. There is not much modification in robot platform, for instance, computer vision tool is additionally attached in body of robot and implementation in robot software consents to manipulate.

Following the concept of robot's awareness, developers in [11] represented a collision-free interaction model which is not only control the robot in collision-avoidance path, but also perceive information from human's activities. To support the mentioned requirements, a context-aware collision avoidance interaction system design that consists of sensing module, path planning module and context-aware human pose recognition module was mainly described. In the similar manner, some researchers [12] suggested the

Table 1: The summary of the state-of-the-art research topics.

Classifications	Author(s)	Methodology	Advantage(s)	Limitation(s)
Collision-free approach based on human-in-loop in cyber-physical system (CPS)	Nikolaos N. et al. [9]	The proposed CPS architecture enables collision risk assessment on the scale of millisecond regarding the triggering of safety policies	(i) Low cost and efficient time performance (ii) Method of human detection and enabling reaction signal	(i) Loading status may impact on robot's action (ii) Relationship between response time and image processing is unknown
	Mohammad S. et al. [10]	The proposed framework from data fusion between laser scanner and IMU to calculate the human-robot minimum distance on-the-fly is investigated	(i) Accuracy and reliability are manageable for collision avoidance success	(i) A limited number of industrial tasks was carried out and residual vibration from robot's motion which acted on results, was not evaluated
Collision-free approach based on environmental context-awareness in CPS	Hongyi L. et al. [11]	The context-aware collision-free system with sensing module for path planning based on human pose recognition is introduced	(i) Detecting potential collision and planning a path to reach target simultaneously (ii) Be able to distinguish human pose and assembly context	(i) Burden computation, an exact human pose recognition algorithm and various assembly sequence are challenges
	Yingzhong T. et al. [12]	A universal control system which allows an operator to communicate his motions to the robot manipulator, is proposed on the self-adaption workspace mapping method	(i) No need to find parameters by trial-and-error (ii) It adapts to different operators and robots in workspace	(i) The recognition and classification of human movements were not focused (ii) The effective distance between operator and system was not discussed.
	Zong C. et al. [13]	A study for the adaptability of the tracked robot in complex working environment is explored. It includes the mechanical structure, static stability in three terrains for human-robot interaction	(i) Appropriate dimension, good mass distribution and limited velocity is advantageous to maintain the system stability on terrains	(i) Load capacity and financial effectiveness are crucial to investigate
	Wang H. et al. [14]	The investigation on improving the performance of RFID robot system by anticollision scheme is exemplified. The tag collisions in the current slot are detected by proposed method, then further resolve each small tag collision to enhance system	(i) This approach is beneficial to boost the moving speed and identification reliability of the RFID robots in complex environments	(i) The solution did not fully consider in the context of collaboration, stability or dynamical control (ii) The phenomenon of weak signal, tags on multi-RFID robots and identification efficiency might occur in practice
	Zong C. et al. [15]	The dynamic process of climbing stairs for the tracked mobile robot is analysed by reason of on the novelty of mechanical structure and working principle	(i) The feasibility of design and flexible motion could be gained in unknown environment	(i) The advanced algorithms should be considered to deal with different sizes of stairs

Table 1: Continued.

Classifications	Author(s)	Methodology	Advantage(s)	Limitation(s)
Collision-free approach based on mathematical computing control in CPS	Andrea M. Z. et al. [16]	An avoidance strategy based on depth camera that suggests the robot alternative paths to be traversed, is achieved both collision free and minimum traversing time	(i) This scheme could predict unintended contacts with operator and maintain the speed of robot as much as possible close to its max value	(i) The traffic conditions should be studied more if ethernet connection is utilized
	Mingcong C. et al. [17]	An artificial potential field-based novel model predictive control path replanner is implemented to provide ample space and sufficient time for proper steering/accelerate/brake in such hazardous scenarios	(i) The proposed method is still deemed capable of tracking aggressive collision-free trajectories while maintaining vehicle stability	(i) A model of four-wheel-independently-actuated is not practical
	Xiangkun H. et al. [18]	A novel emergency steering control strategy consisting of decision-making layer and motion control layer performs a collision avoidance maneuver	(i) The physical limits of driving actuators and nonlinear factors are included	(i) Human's behaviour was not concerned
	Joseph F. et al [17]	A new control structure using model predictive and feedback controller with tire nonlinearities provides firstly collision avoidance ability, then temporarily violate stabilization criteria	(i) All of vehicle's performance capability are utilized to avoid an accident (ii) Prioritizing targets are defined	(i) Be inappropriate with cargo-transportation vehicle
Collision-free approach based on human emotion and activity recognition in CPS	Huang X. et al. [19]	Due to the fundamental emotion modulation theory and the neural mechanisms of generating complex motor patterns, a model of emotion generation and modulation to train a recurrent neural network for robot control to perform goal-directed tasks	(i) The emotion-modulating method is able to control manipulator with higher accuracy and faster learning rate	(i) Various faces with many emotions involve the excellent training process
	Guo S. et al. [20]	A novel idea for nonlinear multiview Laplacian least squares (MvLL) which construct a global Laplacian weighted graph in order to introduce category discriminant information as well as protect the local neighbourhood information, is proposed.	(i) The effectiveness and robustness of MvLL approach is approved although the tasks of multipose and multifeature are taken	(i) The largest disadvantage of this method is the high time complexity
	Zheng E. et al. [21]	The new musculoskeletal-based-method manipulated by the electrical Impedance Tomography (EIT) signals for continuously estimating wrist flexion/extension angles is mentioned in the field of wearable robot	(i) The model-based method performed better with small training data sizes	(i) It is limited in extracting motion information on large data and multi-degree-of-freedom

Table 1: Continued.

Classifications	Author(s)	Methodology	Advantage(s)	Limitation(s)
Collision-free approach based on skill-learning/skill-transfer method in CPS	Su H. et al. [22]	A novel methodology by integrating the cognitive learning techniques and the developed control techniques, which allow the robot to be highly intelligent to learn senior surgeons' skills and to perform the learned surgical operations in semiautonomous surgery, was discussed	The control algorithm does not only provide the learning ability of the human operation skill from multiple demonstrations on a specific task, but also can transfer the learned motion from open surgery by guaranteeing the robot constraints	More complicated motions entail advanced sensors and burden computation
	Su H. et al. [23]	An improved human-robot collaborative control scheme was proposed in teleoperated minimally Invasive surgery scenario	The contributions are not only the improvement of surgical task accuracy and robot constraint, but also the computation efficiency without trajectory planning	Adding one more force sensor for external forces sensing should be conceived and performed with the physical interaction between the surgical tip and the organs
	Su H. et al. [24]	The swivel motion reconstruction approach was applied to imitate human-like behaviour using the kinematic mapping in robot redundancy in this research	The algorithm gains the highly online regression prediction for accuracy enhancement and fast computation	It is important to integrate both human upper limb kinematic models and joint limits
Collision-free approach based on data fusion for navigation method in CPS	Yang Q. et al. [25]	A novel approach of outdoor localization with 3D-laser scanner is proposed to solve the problem of poor localization accuracy in GPS-denied environments. A path planning strategy based on geometric feature analysis and priority evaluation algorithm is also adopted to ensure the safety and reliability of mobile robot's autonomous navigation and control	The robot has high accuracy of localization without GPS so that the mean error of position is 0.1 m and the mean error of path angle is 6° in the experiment. The function of obstacle avoidance includes static obstacle avoidance, dynamic vehicle avoidance and going through narrow regions	The mechanical structure of mobile platform does not guarantee to overcome any outdoor environment
	Sanders D. et al. [26]	The purpose of this investigation is to study the effect on time to complete a task depending on how a human operator interacts with a mobile robot. This kind of interaction utilizes two teleoperated mobile-robot systems, three different ways of interacting with robots and several different environments	It may perform better without a sensor system to assist in more complicated environments. Sometimes, it performs better with a camera mounted on the robot compared with premounted cameras observing the environment	It relies heavily on visual feedback and experienced operators
	Chen D. et al. [27]	A control framework was used and consisted of two levels: one was a decision level to give the possible positions of all nodes in sensor networks, while the other was a control level to move along the edge of obstacles such that the problem of obstacle avoidance can be transformed into a coordination problem of multiple robots	The proposed control approach can guide the mobile robot to avoid obstacles and deal with the corresponding dynamical events so as to locate all sensor nodes for an unknown wireless network	If the number of obstacles increases, the average localization errors between the actual locations and the estimated locations significantly increase

Table 1: Continued.

Classifications	Author(s)	Methodology	Advantage(s)	Limitation(s)
Collision-free approach based on trajectory online adaptation in tele-robot	Luo J. et al. [28]	An innovative method of human motion prediction according to an autoregressive model for teleoperation was motivated. The robot's motion trajectory could be updated in real time through updating the parameters of the proposed model	This approach combines both the prediction of human movement as a feedforward component and a virtual force as feedback	The actively interactive performance of robot as well as the existing trouble in time delay should be considered
	Jing L. et al. [29]	A hybrid shared control approach based on EMG signals sensor and artificial potential field is invented to avoid obstacles owing to the repulsive force and attractive force from human perception	It provides an alternative force feedback solution along with muscle activation and human's control of intention and prediction	The robustness and long distance control of the proposed work could be noticed

universal control system that naturally releases an object manipulation mission from combining the human's gesture to robot manipulator. The advanced functions, for example recognition and classification of shoulder, elbow, wrist or tip of fingers are utilized to control the robot end point. By providing the learning abilities for robot after some iteration processes, a cooperative robot for pick-and-place tasks becomes more intelligent in its workplace. Toward an optimal solution, the research on collaborative robot [16] investigated an avoidance strategy that generated the alternative trajectory to possibly traversed. The superior outcomes are both to prevent collision and to minimize travelling time. Exploiting information receiving from these sensors properly, the robot controller lonely decides motion planning which is the best option in the presence of operator.

Another research topic of safety human-machine interaction is the analysis of dynamic characteristics so as to give a final decision by itself in an emergency case. For these circumstances, a hierarchical model predictive control method was depicted in [17] for four-wheel independent-driving vehicle. An integrated framework that comprises the artificial potential field module for path replanner and feedback compensation control module for path follower, is still capable to track the collision-free trajectories in the ill-conditioned states and supervise the other driving behaviours on the neighbour lane. To deal with uncertain factors in driving actuators and unexpected problems in emergency steering situation, a decision-making layer is implemented into the hierarchical control architecture [18]. The risk indexes associated with collision and destabilisation, are continuously estimated in threat assessment model. An alternative approach has explicitly incorporated vehicle stabilization into path tracking and collision avoidance framework [17]. Sometimes, it permits that the stable motion of vehicle could be violated temporarily if needed to keep away from potential collisions. As a result, this method differs from any others since prioritizing collision avoidance is higher than.

Though, most of studies does not focus on interaction between autonomous grounded vehicle and human while there is a considerable increasing number of automated solutions in e-commerce, logistics and supply chain. In general, when mobile robot or autonomous vehicle leaves research laboratory and join in manufacturing environment, it must be able to deal with emergency circumstances which occur suddenly. Some of them might necessitate manoeuvrings, i.e., emergency collision-free that requires short time response and maintain vehicle stability. The techniques of emergency collision avoidance for autonomous vehicle are demonstrated in [34].

The situation discussed in this paper is that in which a human interacts with a machine, where the robot is equipped with intelligent awareness to evade concurrences. The engine must determine which stop policies are proper while still preserving the balance and keeping the freight undamaged. By investigating the theory of a mass and spring system, the constraints needed to stabilize the whole structure are achieved robustly. Using the actual context of a distribution centre, where workers are obliged to share their workspace, the automated guided vehicle is employed as the platform to prove the proposed approach. Some smooth motion profiles are used in this hardware test to verify the effectiveness and success of our policy.

3. Problem Statement

The target hardware in our research [35] is based on the automated vehicle shown in Figure 1, which could track a reference trajectory or move freely. Its mission is to lift up the shelf, bring cargo to its destination and set the shelf down. Depending on the applications, navigation tools (radio frequency identification, laser sensor or magnetic guide sensor) are additionally attached to the platform. It can work autonomously in a warehouse while the operator stays along distance away. Nevertheless, in developing countries or in some scenarios where a man needs, without a stop policy, the availability of a machine presents nearby, which may cause an unexpected accident as in Figure 2.

We assume that m_1 and m_2 are the mass of the machine hardware and freight, respectively. Once the robot elevates

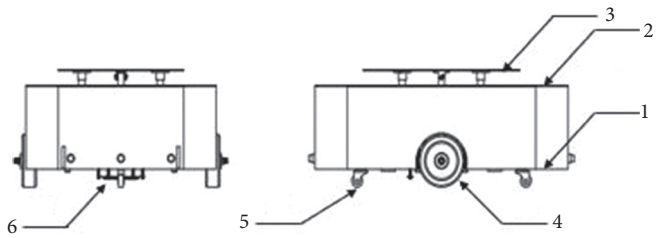

Figure 1: The illustration of our platform, which comprises (1) base, (2) upper cover, (3) lifting part, (4) actively driving wheel, (5) caster wheel, and (6) sensors (line tracking, magnetic tracking and so on).

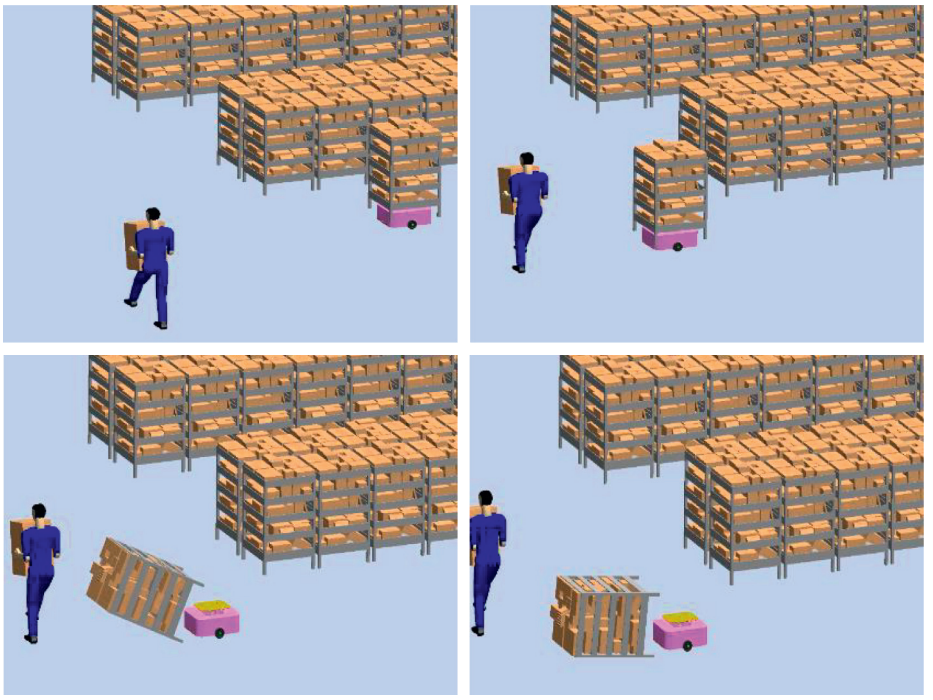

Figure 2: Simulation of physical collision between human and robot sharing the same workspace (see in http://tiny.cc/pawrgz).

the shelf, the two become a rigid body. Without loss of generality, the freight m_2 is connected to the frame via two springs with stiffnesses of k_1 and k_2. The whole modelling procedure is described in Figure 3.

tTo govern the dynamics characteristic, the interacting forces on the system are examined in Figure 4. If the other forces, such as friction forces, exist, they can be ignored. $\vec{\mathbf{v}}$ is the velocity of the vehicle for the same direction of movement. $\vec{\mathbf{F}}_{\mathbf{qt}}$ is the inertial force from the vehicle to the cargo. The state variable $\mathbf{x}$ of the system denotes displacements of each element in vector form: $\mathbf{x} = [\, x_1 \;\; x_2 \,]^T$. Applying Newton's law, the relationship among them can be realized as.

$$m_2 \vec{\mathbf{a}}_2 = k_1 \vec{\mathbf{x}}_2 + k_2 \vec{\mathbf{x}}_2 + \vec{\mathbf{F}}_{\mathbf{qt}}. \tag{1}$$

(1) is rewritten in the positive direction,

$$m_2 a_2 = -k_1 x_2 - k_2 x_2 + m_1 a_1, \tag{2}$$

$$\Leftrightarrow m_2 \ddot{x}_2 = -k_1 x_2 - k_2 x_2 + m_1 \ddot{x}_1. \tag{3}$$

The above equations are related to the time domain. To convert them into the frequency domain, by taking the Laplace transformation, we obtain the following

$$m_2 s^2 X_2 = -k_1 X_2 - k_2 X_2 + m_1 s^2 X_1, \tag{4}$$

where X_1, X_2 mean the Laplace transformations of. x_1, x_2

By using mathematical manipulation, the related constraints in the proposed model are expressed as

$$X_2 = \frac{m_1 s^2 X_1}{k_1 + k_2 + m_2 s^2}, \tag{5}$$

or

$$\frac{X_2}{X_1} = \frac{s^2}{s^2 + \omega_n^2}, \tag{6}$$

ω_n is the natural frequency of the damped system.

If the base X_1 is utilized precisely, the performance of mass X_2 can be measured via (4). In the initial issue, the

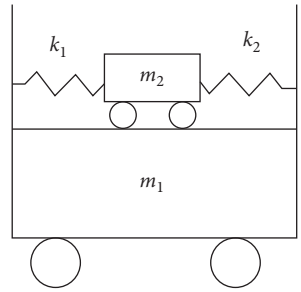

Figure 3: Model of the vehicle and cargo that is assumed in standby status.

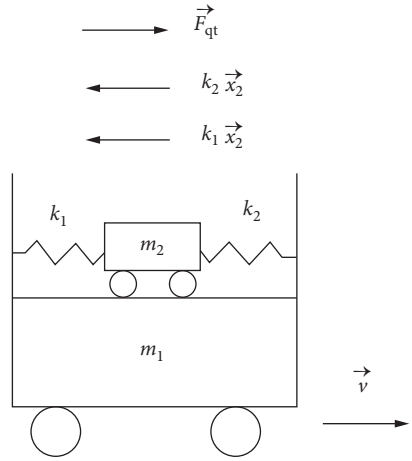

Figure 4: The forces acting on the model are estimated simply in deceleration status.

velocity of X_1 is governed by the trapezoidal scheme shown in Figure 5. Three phases occur for this shape: acceleration, constant speed and deceleration. We are focused on the relationship between the deceleration period and stop status.

$v_{\max}, A_{\max}$: maximum value of the velocity v and acceleration At_a, t_c, t_d: time period of acceleration, constant speed and deceleration, respectively

t_0, t_1, t_2, t_3: time slice at the beginning of acceleration, constant speed, deceleration and end of motion, respectively.

Analysing the above equations, the natural characteristic of the overall system is revealed through poles and zeros which are depicted in the real-imagine coordinate as Figure 6. Since these points locate at the vertical axis, they are usually symmetrical about the horizontal axis.

Poles: $k = 1, 2, 3, \ldots$

$$s_{P_{1,2}} = \pm j\sqrt{\frac{k_1 + k_2}{m_2}} = \pm j\omega_n = \pm j2\pi f_n. \tag{7}$$

Zeros:

$$s_{Z_{1,2}} = \pm j\frac{2\pi k}{t_3 - t_2}. \tag{8}$$

Theoretically speaking, the autonomous system tends to oscillate if the system states are at the poles. In detail, when the conditions in (5) are satisfied, the unexpected vibration might occur and ascend inside this system. As a result, the incident event could cause harm to workers quickly.

4. Proposed Stop Strategy

To overcome these challenges, a pole placement for cancelling the unstable points is introduced. The advantages of this approach are that it suppresses the residual vibration, carries out the tuning rule regarding physical factors and the actuator specification, and does not require the exact information of the model. Therefore, free-vibration motion can be achieved in a robust manner.

4.1. Robust Pole Placement Technique. Our motivation is to present the novel approach for stable control according to the analysis of system state. Deriving from the idea of pole placement technique, the pole-zero cancelation method is applicable if the zero points are duplications of the locations of the poles. In Figure 7, the outcome of this work is to identify the condition for relocating zero points to positions of poles. By substituting into (5)-(6), the vibration-less conditions are as follows.

$$\sqrt{\frac{k_1 + k_2}{m_2}} = \frac{2\pi k}{t_3 - t_2}, \tag{9}$$

$$\Leftrightarrow T_3 = \frac{2\pi k}{\omega_n}, \tag{10}$$

$$\Leftrightarrow f_n T_3 = k. \tag{11}$$

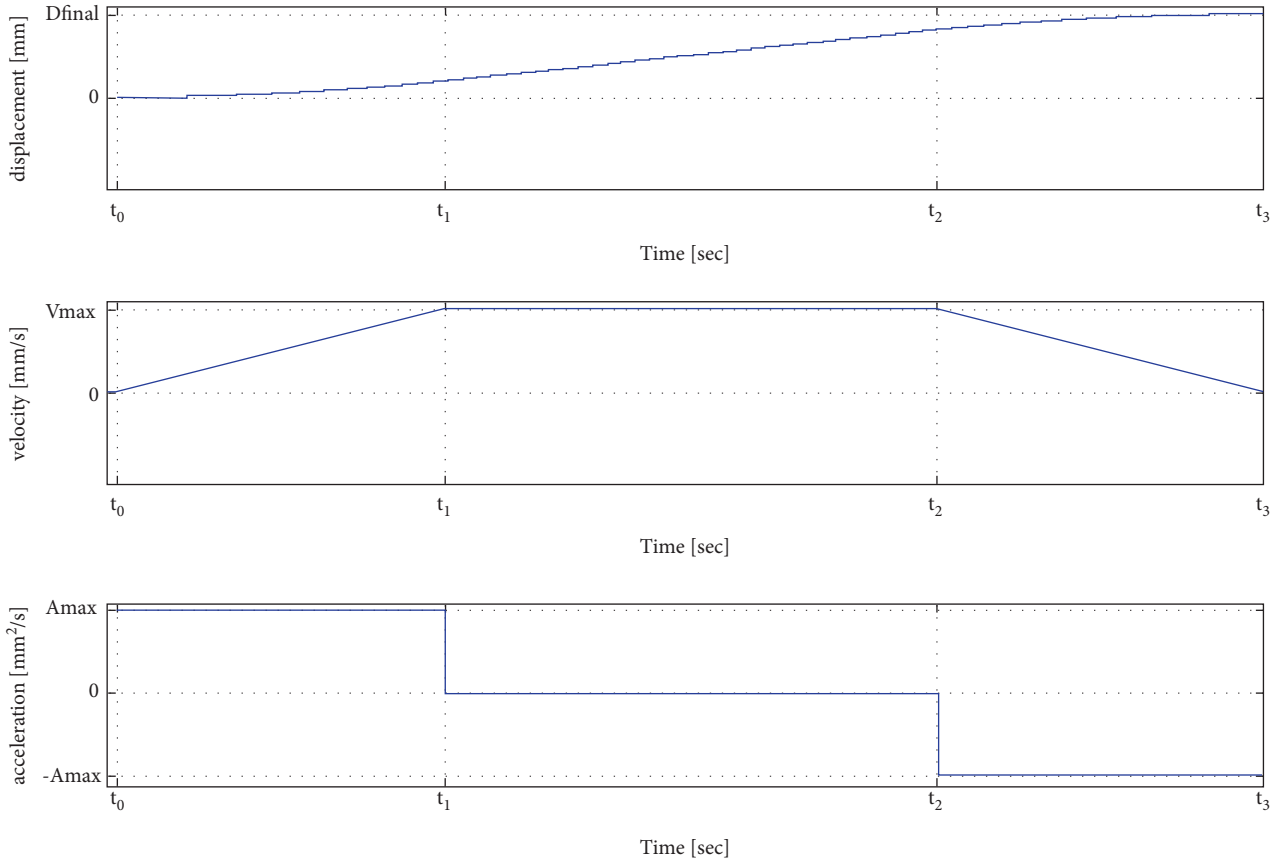

Figure 5: Motion profile of the velocity and acceleration in the trapezoidal strategy.

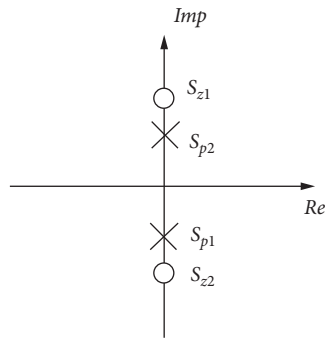

Figure 6: The poles and zeros are placed in the imaginary plane; *o*: zero, *x*: pole.

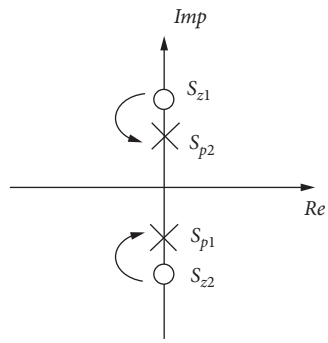

Figure 7: The free-vibration motion by the pole placement technique; *o*: zero, *x*: pole.

$$V(t) = \ddot{x}(t) = \begin{cases} \frac{1}{2}J_{\max}t^2 + V_o, & 0 \le t < t_1, \\ A_{\max}(t - t_1) + V_1, & t_1 \le t < t_2, \\ A_{\max}(t - t_2) - \frac{1}{2}J_{\max}(t - t_2)^2 + V_2, & t_2 \le t < t_3, \\ V_3, & t_3 \le t < t_4, \\ -\frac{1}{2}\frac{J_{\max}}{\gamma^2}(t - t_4)^2 + V_4, & t_4 \le t < t_5, \\ -\frac{A_{\max}}{\gamma}(t - t_5) + V_5, & t_5 \le t < t_6, \\ -\frac{A_{\max}}{\gamma}(t - t_6) + \frac{1}{2}\frac{J_{\max}}{\gamma^2}(t - t_6)^2 + V_6, & t_6 \le t < t_7. \end{cases} \tag{12}$$

In the physical view, when duration T_3, from t_2 to t_3, is the integer multiples of the period of oscillation, the vibration suppression is entirely effective after the vehicle completes its motion. This key constraint guarantees that there is no sudden vibration during the deceleration stage and that the vehicle actively breaks at the specified position. From this idea, various stop profiles are researched to determine which is proper for different cases.

4.2. Stop Profiles. The criteria to rate the proper profile are able to suppress the vibration of both the vehicle and cargo; the policy of the generating mechanism depends on the system constraints and ensures the real-time performance. First, the trapezoidal profile is chosen due to its simplicity but effectiveness, and it does not cost much in terms of the timing generation. Later, without loss of generality, the strategy is exerted on numerous profiles for comparison. If the initial velocity V_0 is given, then the expression of the asymmetric S-curve speed profile [36] can be manifested as follows:

With

$$V_1 = \frac{1}{2}J_{\max}t_1^2 + V_0, \tag{13}$$

$$V_2 = A_{\max}(t_2 - t_1) + V_1, \tag{14}$$

$$V_3 = A_{\max}(t_3 - t_2) - \frac{1}{2}J_{\max}(t_3 - t_2)^2 + V_2, \tag{15}$$

$$V_4 = V_3, \tag{16}$$

$$V_5 = -\frac{1}{2}\frac{J_{\max}}{\gamma^2}(t_5 - t_4)^2 + V_4, \tag{17}$$

$$V_6 = -\frac{A_{\max}}{\gamma^2}(t_6 - t_5) + V_5, \tag{18}$$

$$V_7 = -\frac{A_{\max}}{\gamma}(t - t_6) + \frac{1}{2}\frac{J_{\max}}{\gamma^2}(t - t_6)^2 + V_6, \tag{19}$$

$$\tau_m = \frac{V_{\max}}{A_{\max}}, \tag{20}$$

$$t_j = \beta\tau_m, \tag{21}$$

$$t_a = (1 - \beta)\tau_m, \tag{22}$$

$$J_{\max} = \frac{A_{\max}}{t_j}. \tag{23}$$

In Figure 8, the asymmetric S-curve motion profile of the mobile base is written with the unit step function $u(t)$. Totally, there are seven segments with $[t_i, t_{i+1}], i \in \{0, 1, 2, 3, 4, 5, 6, 7\}$. $V_{\max}, A_{\max}, J_{\max}$ are maximum values of velocity, acceleration and jerk correspondingly. V_i is the final value of velocity in the time slice $[t_{i-1}, t_i]$. τ_m is ratio between velocity and acceleration while t_j and t_a are the acceleration/deceleration time and constant acceleration respectively. Thus, equation (12) depicts the time-varying velocity of system. From equations (13) to (19), the components of velocities in each period are identified. The relationship between maximum acceleration and maximum velocity as well as tuning parameters is illustrated from equations (20) to (23).

$$\begin{aligned} s^2X_1 = &-\frac{J_{\max}}{\gamma^2}(t - t_4)[u(t - t_4) - u(t - t_5)] \\ &-\frac{A_{\max}}{\gamma^2}[u(t - t_5) - u(t - t_6)] \\ &+\left(\frac{J_{\max}}{\gamma^2}(t - t_2) - \frac{A_{\max}}{\gamma}\right)[u(t - t_6) - u(t - t_7)]. \end{aligned} \tag{24}$$

Substituting the above into (4), the information of mass m_2 can be measured as

$$s^2 X_2 = -\frac{m_1 J_{\max}\left(e^{-t_4 s} - e^{-t_5 s} - e^{-t_6 s} + e^{-t_7 s}\right)}{m_2 \gamma^2 \left(s^2 + \omega_n^2\right)}. \tag{25}$$

In the time domain, (10) is expressed in time-varying form.

$$\begin{aligned}\ddot{x}_2(t) &= -\frac{m_1 J_{\max}}{m_2 \gamma^2 \omega_n} \times \left[\sin\left(\omega_n\left(t - t_4\right)\right) - \sin\left(\omega_n\left(t - t_5\right)\right)\right. \\ &\quad \left. -\sin\left(\omega_n\left(t - t_6\right)\right) + \sin\left(\omega_n\left(t - t_7\right)\right)\right].\end{aligned} \tag{26}$$

It has been indicated that the performance of a vehicle in lifting cargo m_2 is discoursed via four sine functions. Their mutual characteristics equalize the frequency but shift the phase. To acquire the desired output, these terms of (11) are forced to dismantle each other. In the case where the control algorithm is valuable, the oscillating performance of m_2 approaches zero. The concern in this paper is to develop a policy for stabilizing the movement of a system with different deceleration phases. Again, using the asymmetric S-curve profile, the general conditions needed to eliminate the vibration of cargo are demonstrated.

$$\frac{2\pi k}{\beta \gamma \tau_m} = 2\pi f_n, \tag{27}$$

$$\Leftrightarrow \beta \gamma \tau_m = k T_n, \tag{28}$$

$$\frac{2\pi m}{\gamma \tau_m} = 2\pi f_n, \tag{29}$$

$$\Leftrightarrow \gamma \tau_m = m T_n. \tag{30}$$

From the above results, it is clear that the fluctuation can be destroyed when the motion planning period equals an integer multiplied by the period of natural oscillation. It is desired that at the end of mobile platform movement, the vibration of m_2 is completely cancelled as soon as possible. Some simulations with a trapezoid, an S-curve, and an asymmetric S-curve or without a strategy are shown in Figures 9–12, respectively.

$$\delta_{\mathrm{SPB}} = \frac{V_{\max}^2}{2A_{\max}}(1 + \beta), \quad \forall \beta. \tag{31}$$

Generally, it is critical to find the minimum distance for vehicle to generate the smooth stop profile. If ΔP_i symbolizes the moving distance during a period, later the number of displacements in deceleration duration are expressed as follows:

$$\Delta P_5 = J_{\max} \gamma \left(\beta \tau_m\right)^2 \left(\frac{5}{6}\beta \tau_m + t_a\right), \tag{32}$$

$$\Delta P_6 = \frac{1}{2} J_{\max} \gamma \beta \tau_m t_a \left(\beta \tau_m + t_a\right), \tag{33}$$

$$\Delta P_7 = \frac{1}{6} J_{\max} \gamma \left(\beta \tau_m\right)^3. \tag{34}$$

MDB (minimum distance barrier): the cyber limitation ($\delta_{\min}$) in awareness of autonomous system to decelerate safely and smoothly minimizes to be required.

$$\delta_{\mathrm{MDB}} = \frac{A_{\max} \gamma \tau_m^2}{2}(1 + \beta). \tag{35}$$

In dissimilar profiles, the restrictions of minimum distances are different. Each type exists a predetermined range from vehicle to human which avoid to interrupt.

TPB (trapezoidal psychological barrier): $\beta = 0$

$$\delta_{\mathrm{TPB}} = \frac{V_{\max}^2 \gamma}{2A_{\max}}, \quad \forall \gamma. \tag{36}$$

SPB (S-curve psychological barrier): $\gamma = 1$

APB (AS-curve psychological barrier):

$$\delta_{\mathrm{APB}} = \frac{V_{\max}^2 \gamma}{2A_{\max}}(1 + \beta), \quad \forall \beta, \gamma. \tag{37}$$

4.3. Active Policies with Respect to Safety. In the paper [37], a unified framework that enables a robot to safely and socially reach both a dynamic human and a human group was developed. Basically, the real-world environment around a human is personal space, where people interact only with close objects such as relatives, and a machine is obligated to inviolate this barrier. In further space, named social space, humans will communicate with others, for example, shaking hands and engaging in oral discussion. A machine should not stay in the social space so that humans feel comfortable and safe. Representing the furthest distance, public space is a cyber interval in which humans come across each other. This is a commonly acceptable gap to preserve a complete stop strategy.

To adapt to the virtual spaces around humans, it is indispensable to launch a switching mechanism among the stop strategies. Given a target distance δ, the mechanism initially ranges from autonomous machines to men.

Here, $H = \{h_1, h_2, \ldots, h_n\}$, where h_i is the ith person. The human states of person h_i are regulated as $h_i = (x_i^h, y_i^h, \theta_i^h, v_i^h)$, where (x_i^h, y_i^h) is the position, θ_i^h is the orientation with $-180^\circ \le \theta_i^h \le 180^\circ$, and v_i^h is the linear velocity. For the vehicle, its states are denoted as $\vartheta_i = (x_i^\vartheta, y_i^\vartheta, \theta_i^\vartheta, v_i^\vartheta)$, where its position is $(x_i^\vartheta, y_i^\vartheta)$ and its orientation is θ_i^ϑ, with $-180^o \le \theta_i^\vartheta \le 180^o$.

In Figure 13, Algorithm 1 is utilized whenever an autonomous vehicle carries out a decision before one is made by a human. In this study, the direction a person faces and the location of the right hand or left hand are not our concern. It is noted that the estimation of the relative distance is not the key discussion. We use Kinect digital camera to gain the depth map from the environment, with far distances, and a skeleton option in tracking mode to calculate the current travelling distance. We input the parameters; the values of $\delta_{\mathrm{APB}}, \delta_{\mathrm{SPB}}, \delta_{\mathrm{TPB}}$ are computed in advance. Because of these data, it can be known which stop policy is best to activate.

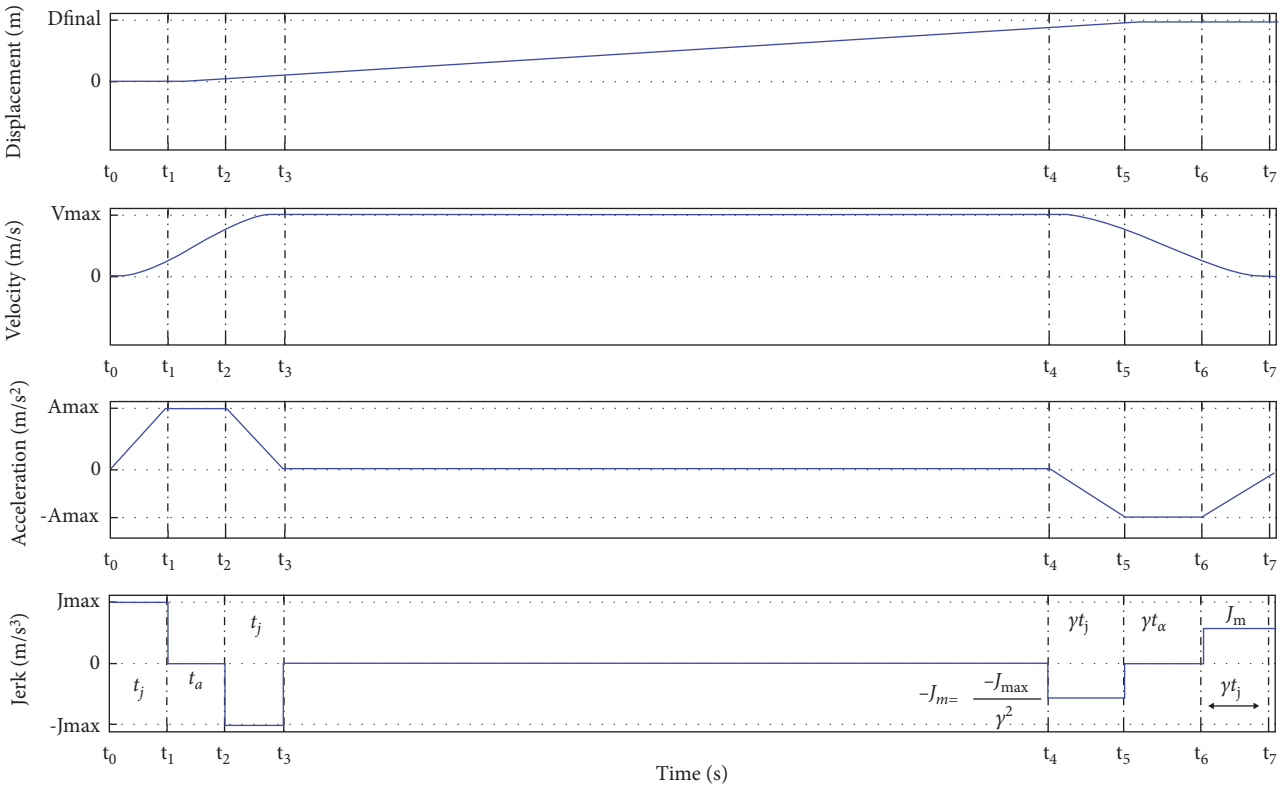

Figure 8: Theoretical motion profile of the asymmetric S-curve.

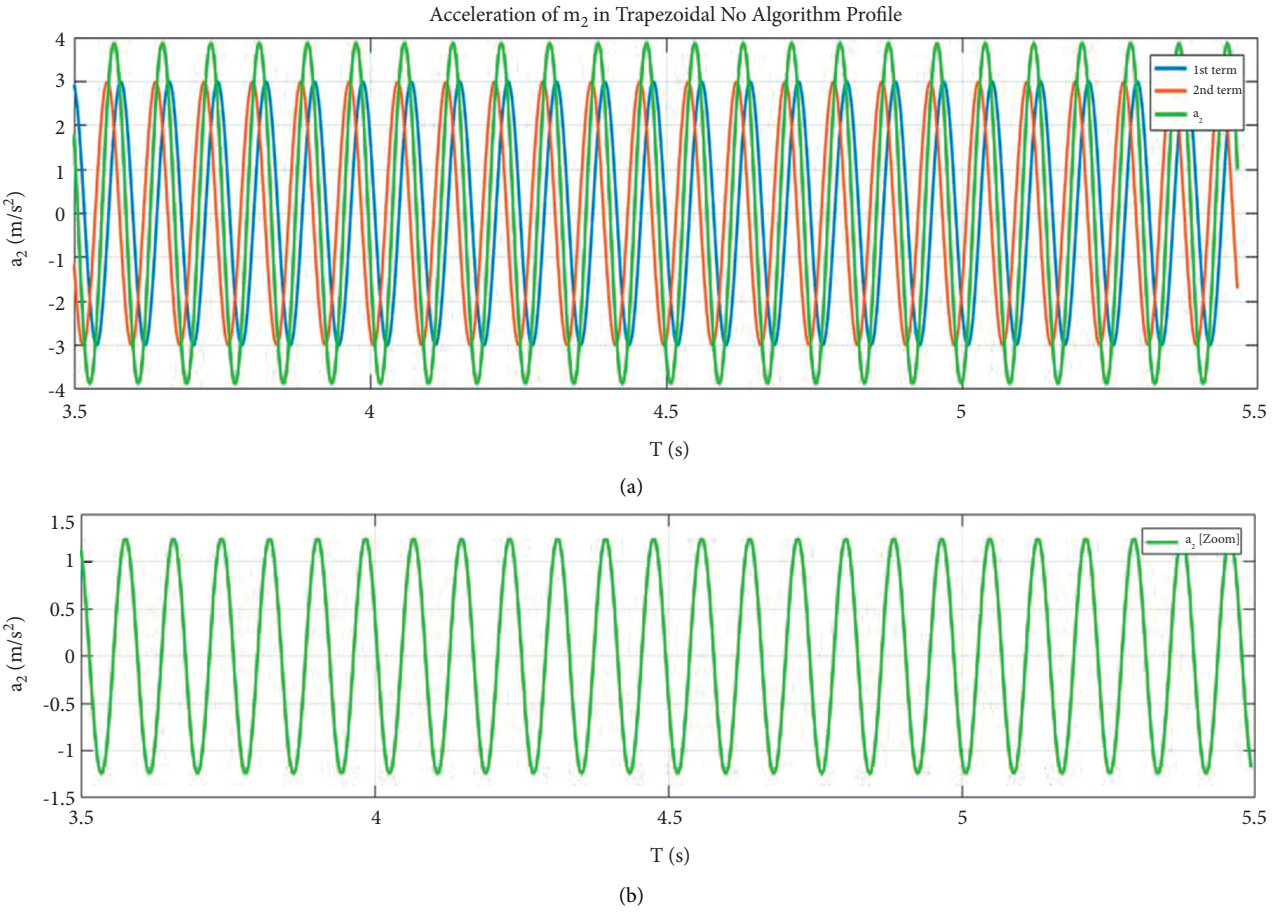

Figure 9: Simulation of the vibration suppression of m_2 (a) and its enlarged plot (b) without a stable strategy. Blue: 1st term, orange: 2nd term, green: m_2 acceleration.

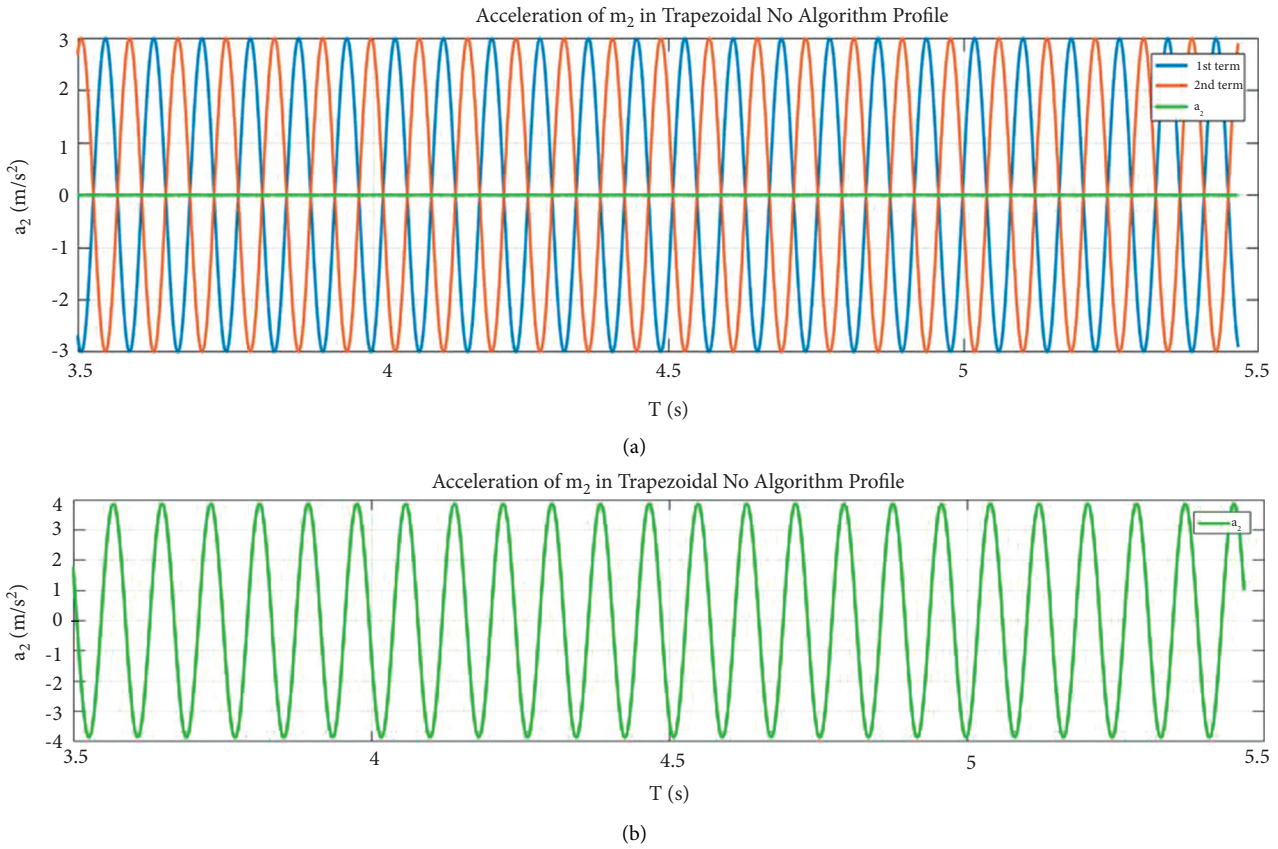

Figure 10: Simulation of the vibration suppression of m_2 (a) and its enlarged plot (b) with the trapezoidal strategy. Blue: 1st term, orange: 2nd term, green: m_2 acceleration.

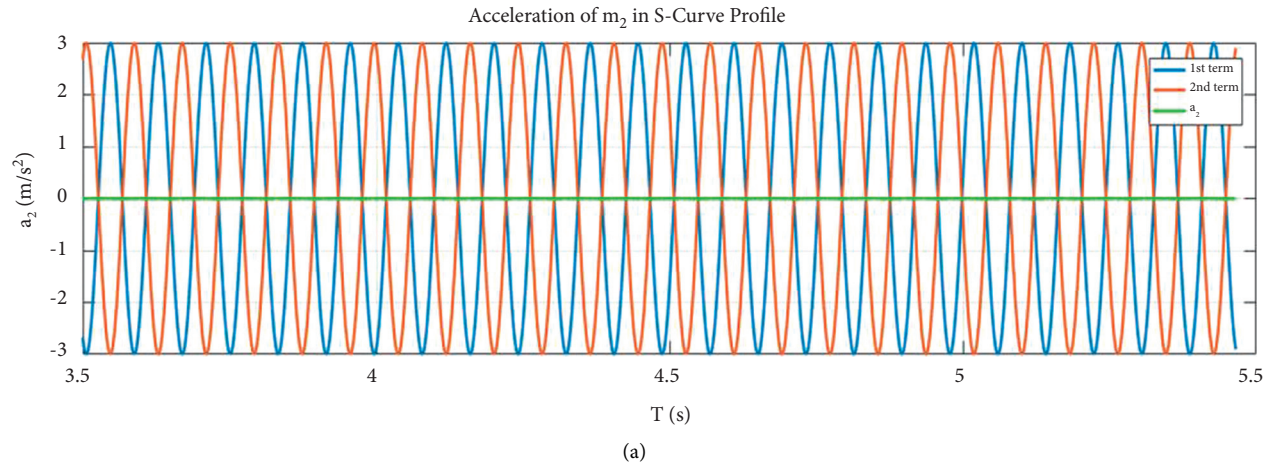

Figure 11: Continued.

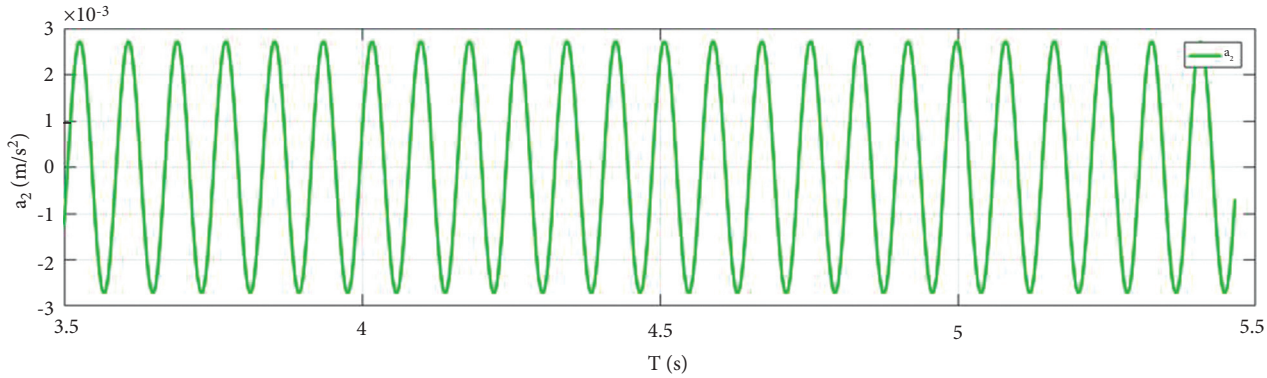

(b)

FIGURE 11: Simulation of vibration suppression of m_2 (a) and its zoom plot (b) with S-curve strategy. Blue: 1st term, orange: 2nd term, green: m_2 acceleration.

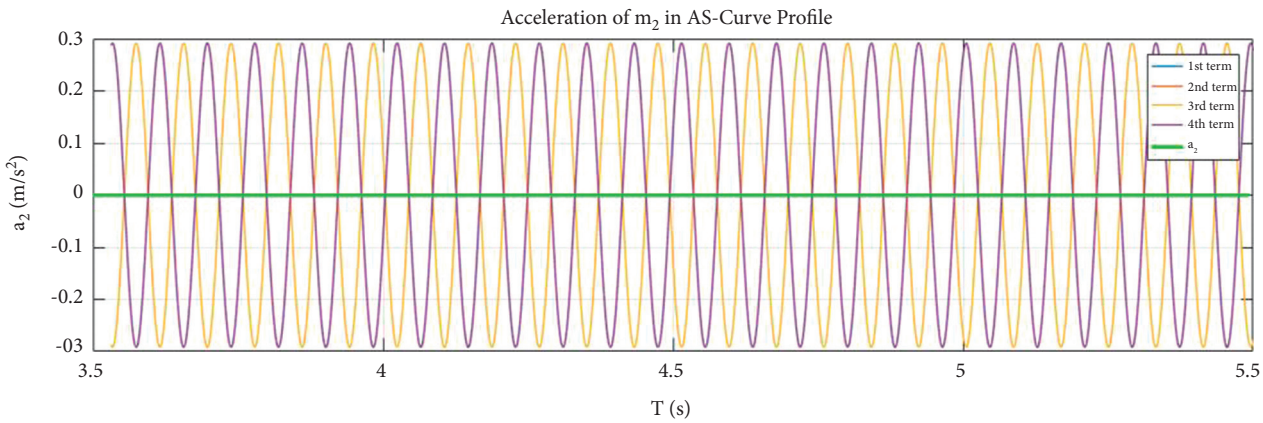

(a)

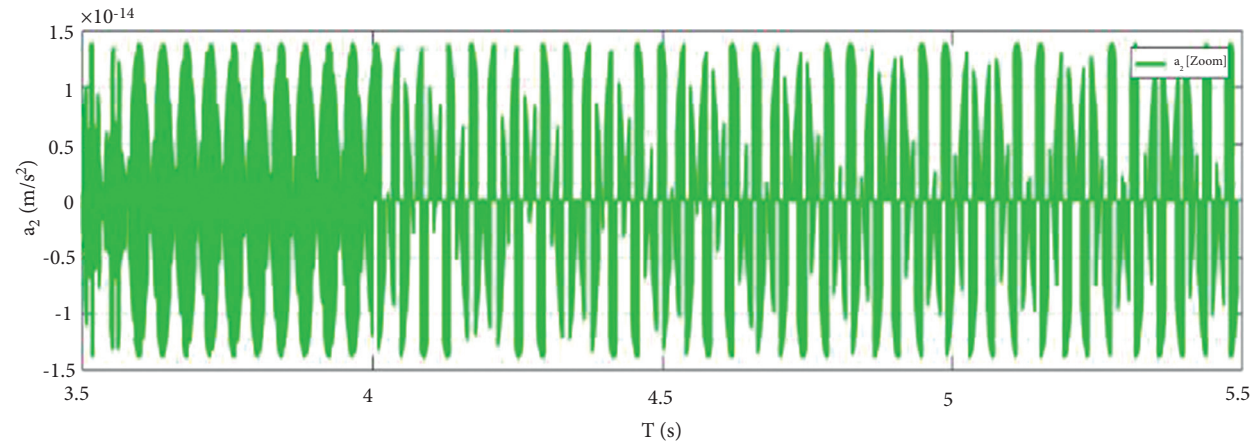

(b)

FIGURE 12: Simulation of the vibration suppression of m_2 (a) and its enlarged plot (b) with the AS-curve strategy. Blue: 1st term, orange: 2nd term, green: m_2 acceleration.

The context of human-machine interaction is illustrated as Figure 14. In this case, a scenario of the possibility humans reaching machines in global coordinate xy consists of v_i^p and v_r denoting velocity vectors of i^{th} person and machine, locations $(x_i^p, y_i^p, \theta_i^p)$ for i^{th} person and (x_r, y_r, θ_r) for machine respectively. Besides, the spaces around human are also described to clarify the approaching zone.

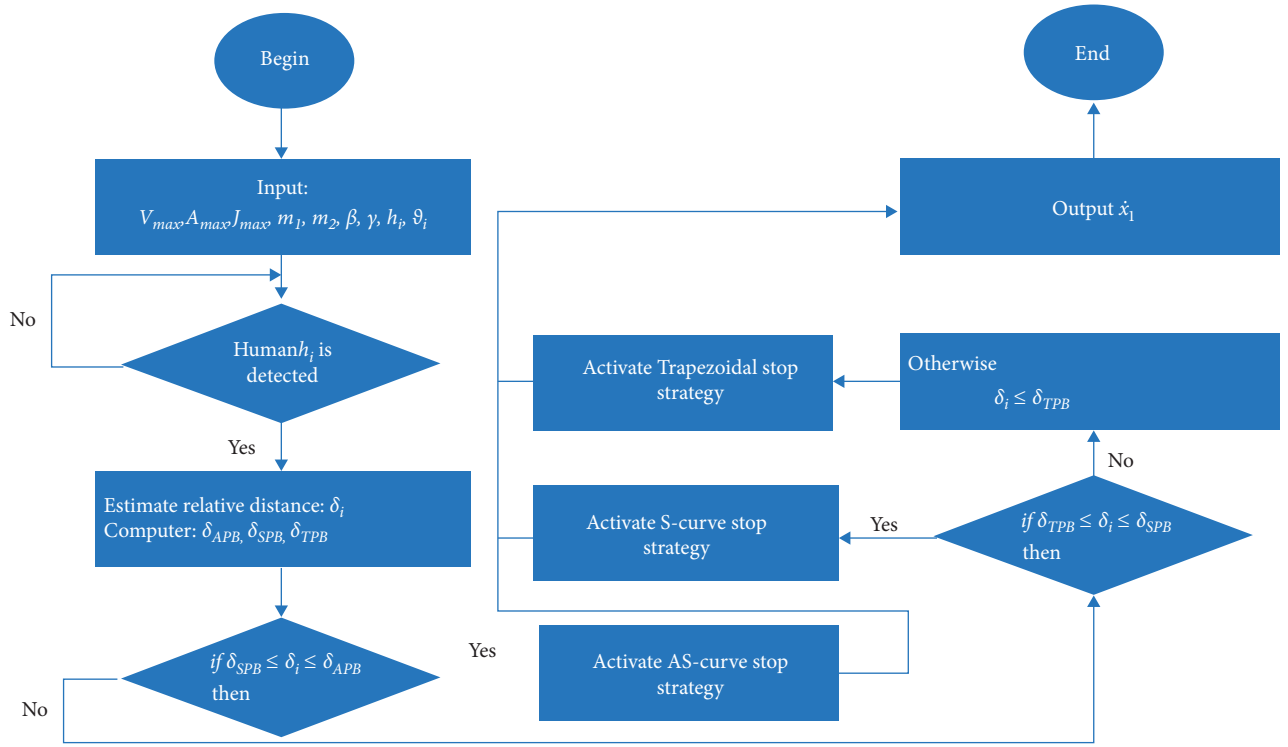

Figure 13: Description of the proposed switching mechanism for stop profile generation.

(i) **Input:** $V_{\max}, A_{\max}, J_{\max}, m_1, m_2, \beta, \gamma, h_i = (x_i^h, y_i^h), \vartheta_i = (x_i^\vartheta, y_i^\vartheta)$
(ii) **Output:** $\dot{x}_1$
(iii) **while** *Human* h_i *is detected* **do**
(1) **Estimate relative distance** δ_i
(2) **Compute** $\delta_{APB}, \delta_{SPB}, \delta_{TPB}$
(3) **if** $\delta_{SPB} \le \delta_i \le \delta_{APB}$
(4) **Activate AS-curve top strategy;**
(5) **else if** $\delta_{TPB} \le \delta_i \le \delta_{SPB}$
(6) **Activate S-curve top strategy;**
(7) **else if** $\delta_i \le \delta_{TPB}$
(8) **Activate Trapezoidal top strategy;**

Algorithm 1: Switching mechanism of stop profile generation.

5. Experimental Validation

In this paper, we suggest two classifications of the experiments. In the first laboratory test, the performance of the separated deceleration scheme needs to be measured. The machine is installed with a consciousness regarding the stop behaviour. The vibration results of different strategies are compared to discover the proper profiles for each situation. The second one tests whether to switch among the strategies in real life.

An experimental platform was setup as in Figure 15 to validate our approach. We developed one practical automated guided vehicle to serve in manufacturing factories or distribution centres. To imitate the reaction of cargo, a mass m_2 connected to a vehicle by means of a linear aluminium ruler is replaced above the lifting component of the vehicle. A sensing board boostXL Texas Instrument, is placed together with the mass to weigh some physical parameters

along the x, y, z axes. To process data in real-time mode, the development kit LaunchPad MSP432P401 R is utilized to record vibrating outputs. This device supports a powerful 32 bit ARM Cortex-M4F microcontroller up to a 48 MHz system clock, 256 KB of flash memory, and 64 KB of SRAM. The data are then transmitted to the embedded computer to acknowledge the system status. To control two servo motors, the TM4C evaluation board and DCS3T-27 driver are used to close the feedback loop. Tiva C series TM4C123 G LaunchPad including the TM4C123GH6PMI microcontroller with two motion control PWM modules capable of generating 16 PWM outputs, two quadrature encoder interfaces, and several driving platforms.

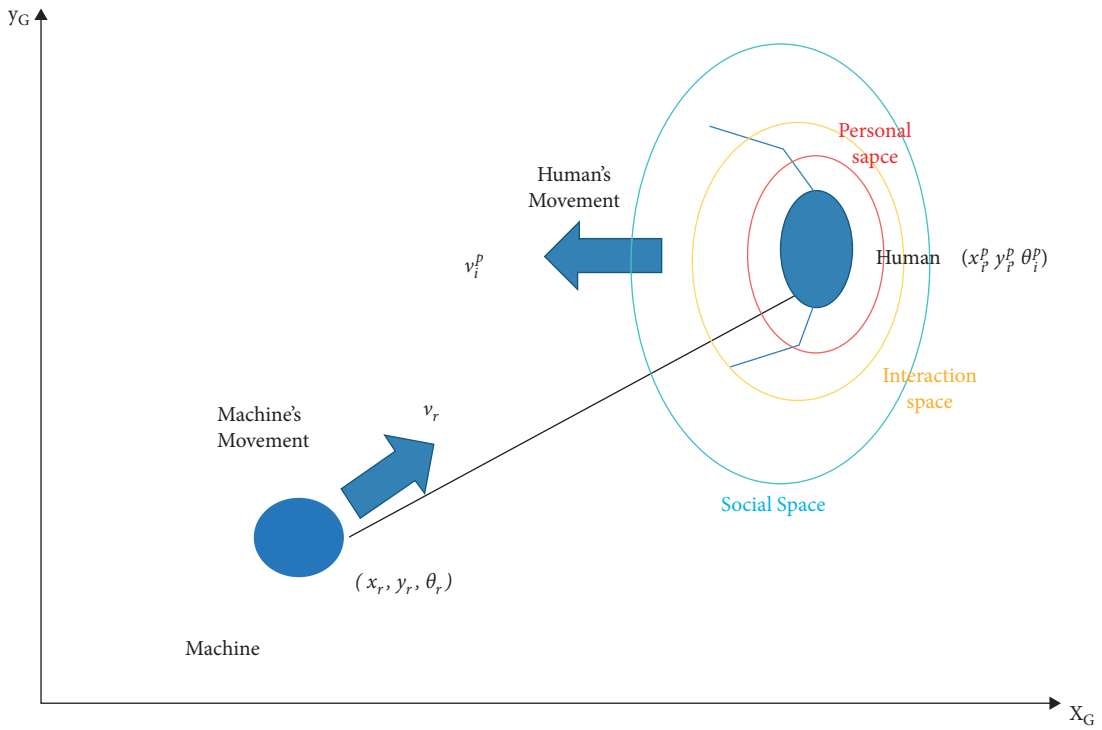

Figure 14: Relative constraints between a human and machine.

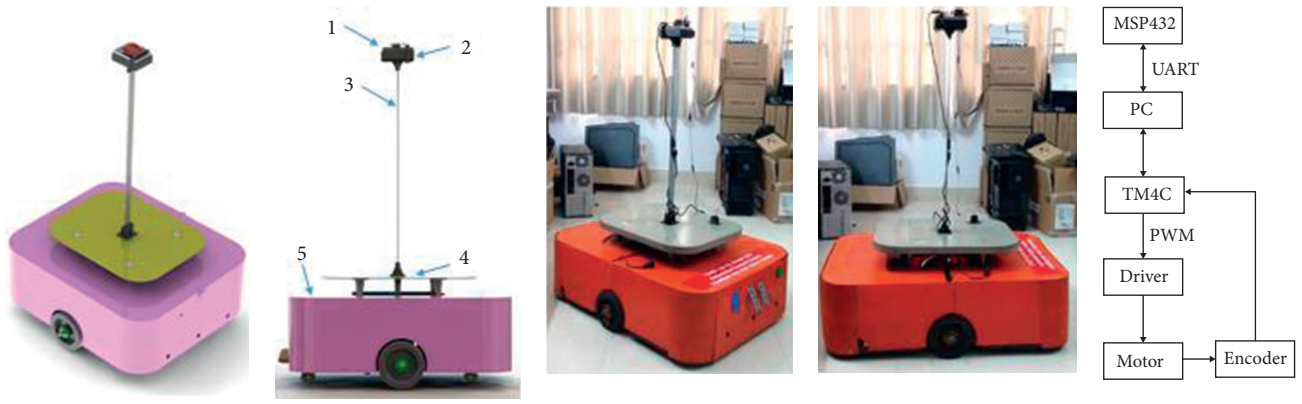

Figure 15: Experimental setup test: (a) virtual 3D view, (b) virtual side view: board sensor[1], m_2 = mass[2], linear ruler[3], lifting component of the vehicle[4], and practical automated guided vehicle[5], (c) real 3D view, (d) real side view and (e) flowchart of the data transmission (see in http://tiny.cc/eewrgz).

In the first validation test, our target is to categorize the performance of these three policies and that without a policy. The separated results in each case should be shown in Figure 16. In the initial stage, because of a sudden break while travelling, the largest swinging wave appears indicating unbalanced movement. Without any policy, the amplitude of the vibration reaches its maximum height after a moment. It takes more time to decline the output variation. Applying the TPB scheme, the result becomes better in terms of a small swing and fast response to suppress vibration. For the effect of the SPB algorithm, the achieved performance is of smaller magnitude for oscillation and suppresses it more quickly. Lastly, the most superior performance of the smallest level of vacillation and the fastest response are achieved by APB scheme while the powerful computation of micro-processor is required. To visualize the differences of their impact, a combined result representing a comparison of the proposed strategies is displayed as in Figure 17. The deep impression on the diminishing vibration of the APB method has been observed. However, its constraints require a machine far enough away to decelerate. On the other hand, the schemes of SPB and TPB satisfy the conditions of vibration suppression while not need more spaces to execute.

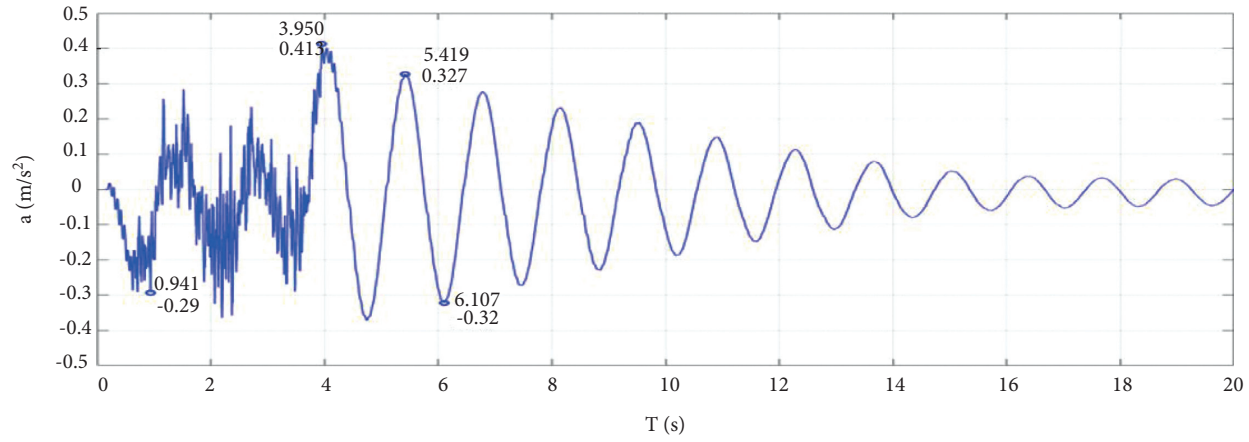

(a)

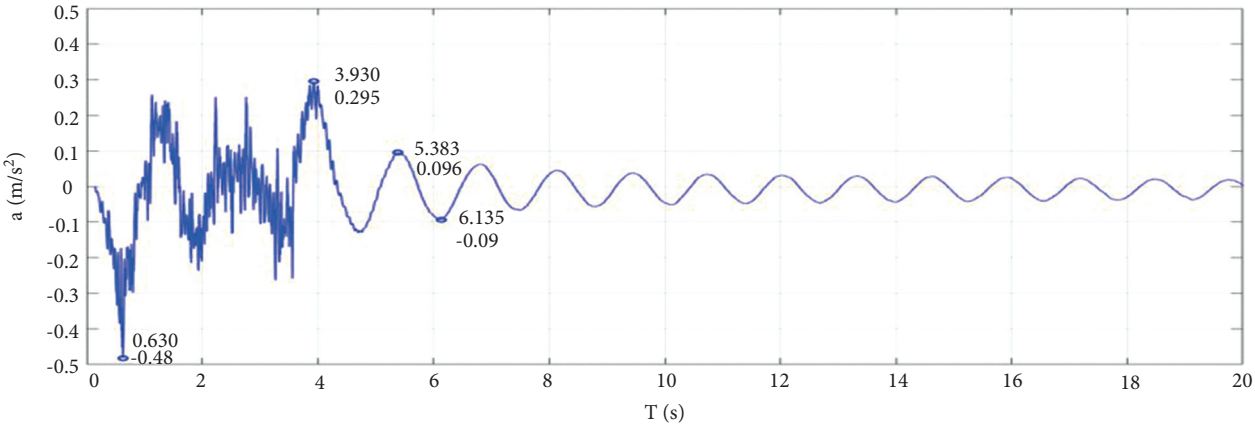

(b)

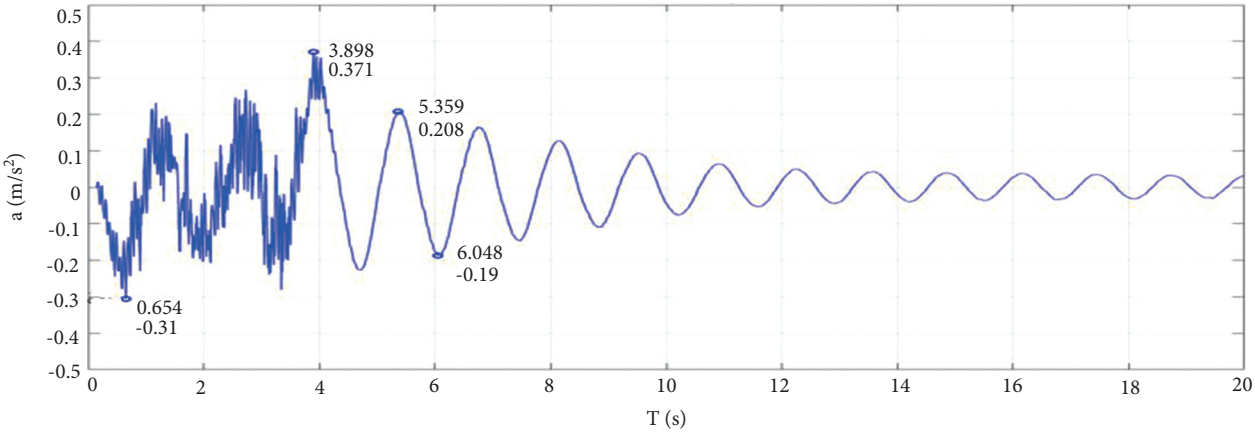

(c)

Figure 16: Continued.

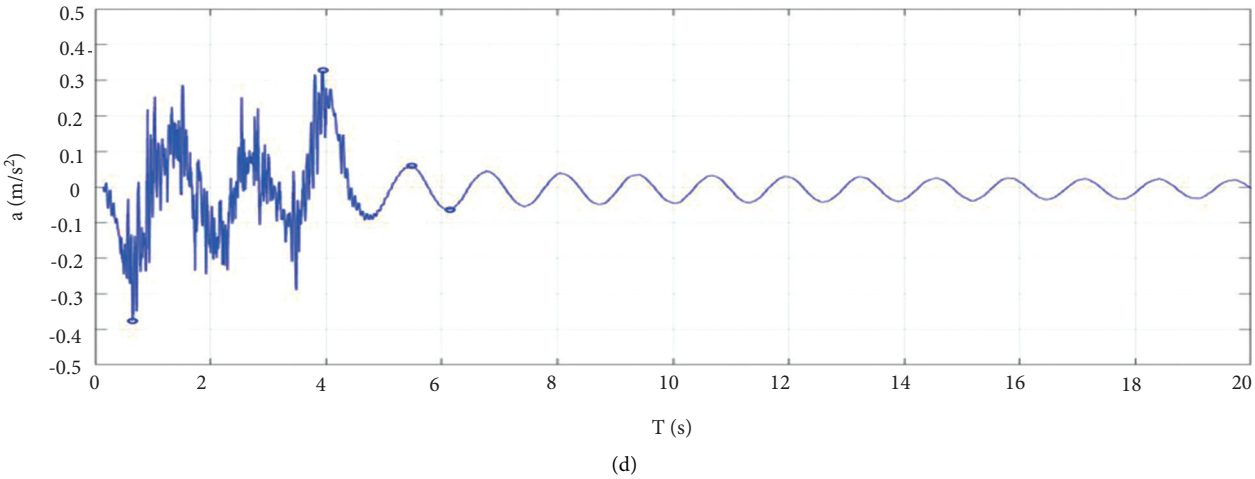

Figure 16: Experimental results of different test scenarios: (a) without a strategy, (b) with SPB, (c) with TPB, and (d) with APB.

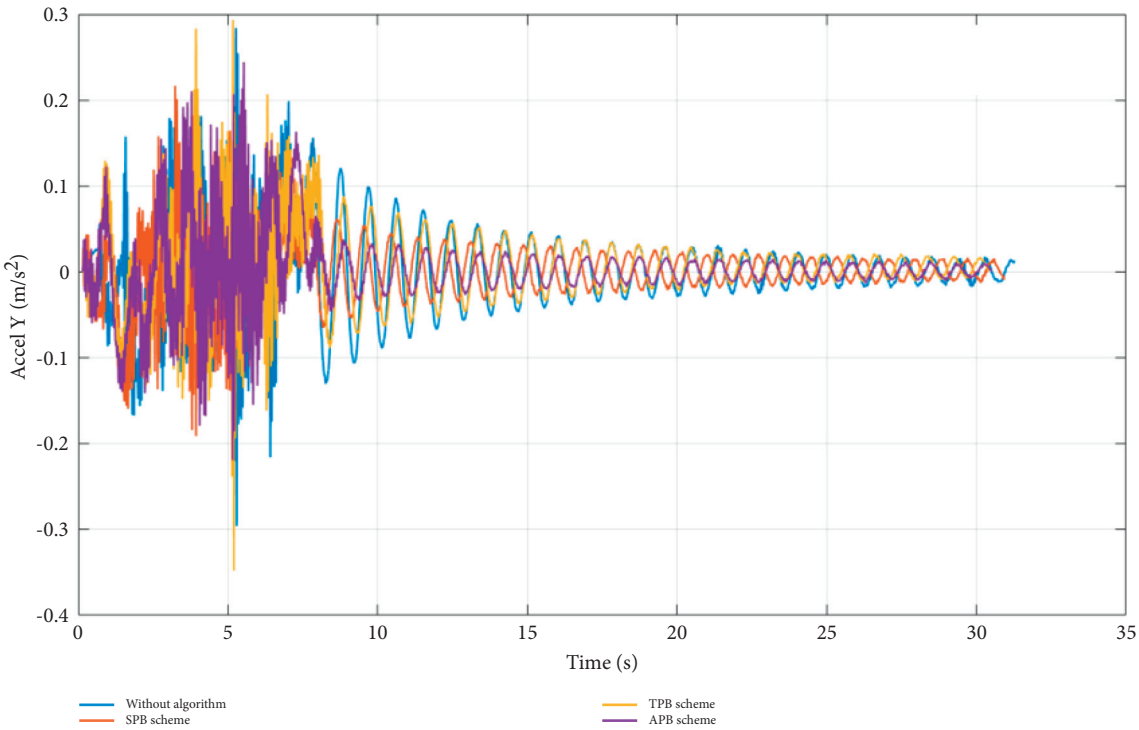

Figure 17: Comparison of test cases with various proposed strategies.

Table 2 reveals the comparative performance for all laboratories. This research regards how fast the oscillation is terminated and how many times the largeness of the oscillation decreases. When the proposed control techniques are not considered, the acceleration of mass m_2 tends to decrease the vibrating magnitude by 1.26 times after 1.47 s. In the primary scheme, TPB helps to lessen the number of times to 1.78 after 1.46 s from the moment of the unexpected stop. In other tests, under the power of the SPB and APB schemes, the vibration declines by 3.07 times and 5.56 times after 1.41 s and 1.27 s, correspondingly. It is concluded that the APB technique can offer the best performance in terms of antioscillation even though it is expected that more space will be required to complete the stop strategy. The others show that a smaller oscillating range and faster response of the system can be attained, and the travelling distance desired by a mobile vehicle can be increased.

Equations (28) and (30) are named E28 and E30, respectively. An autonomous vehicle can be driven with a trapezoidal, an S-curve or an AS-curve speed profile. Depending on the type, the constraints required to address the vibration-free case are dissimilar. For the TPB case, only E30 is able to suppress the oscillation, although it does not violate E28. The APB and SPB schemes are both able to

Table 2: Comparative results of experimental laboratories.

Acceleration of second mass	Min	Max
Without proposed algorithm	−0.323	−0.327
TPB	−0.187	0.208
SPB	−0.09	0.096
APB	−0.064	0.059

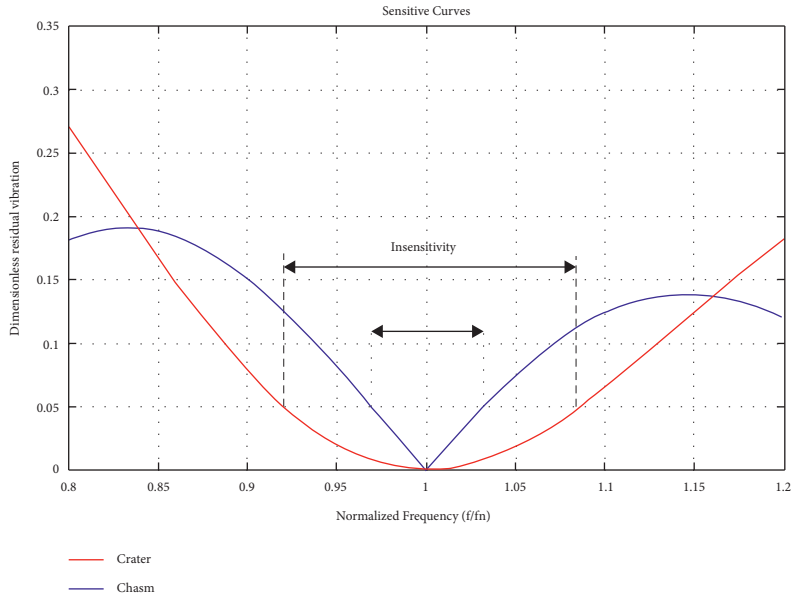

Figure 18: Sensitivity curves of variation in the vibration magnitude against the natural frequency error with $f_n\tau_m = 1.2229$.

operate under the E28 and E30 conditions. After several experiments, it is known that the tolerance of the vibrating frequency in TPB is smaller than that in APB or SPB. The sensitive curve in Figure 18 denotes the variation in amplitude when the estimated natural frequency differs from the practical natural frequency. In this study, it is assumed that the natural frequency error is ±20% of the real value. The motion that satisfies both E28 and E30 is defined as a crater. If it satisfies only one of the above vibration-less conditions, the movement is categorized as a chasm. Notably, the impacts needed to reduce the residual vibration of a crater are larger than those of a chasm.

In general, if the tuning parameters satisfy both E28 and E30, then the residual vibration amplitude will decline in comparison with only E28 or E30 whenever the error modelling is small enough.

6. Conclusions

An active stop strategy with vibration cancelation control and collision avoidance between humans and machines (i.e., material transportation) was proposed in this paper. The antivibration control constraint is analytically well-defined based on a dynamic modelling of a vehicle and cargo. Various profiles for activating the stop policy were inspected, and the specific characteristics of each profile were analysed. In particular, the physical characteristics of TPB, SPB and APB were analytically compared to the case without an active stop planner. From the points of view of smoothness and robustness, both investigated strategies drive the whole platform to halt under flexible motion while the system is constantly stabilized. Owing to the socially aware navigation framework of a mobile platform in dynamic surroundings, we developed a switching mechanism to select the proper profile for different social situations. We certified the effectiveness of the proposed approach through both simulation work and a real-world laboratory test. Clearly, the newly investigated stop method could be incorporated into any path planning technique to enhance the performance of human-awareness of an autonomous system. It is clear that our approach has undergone successful integration such that the robot behaviour is improved to a socially acceptable response, achieving safe restrictions while conserving system parameter constraints.

Compared to the works invented by authors [23], although the interaction force is not mentioned and the natural frequency seems to be difficult to estimate, our study focusses on stable control for the autonomous vehicle. Compared to our previous topic [35], not only the potential human-machine interaction is examined, but also the internal system state is mainly concerned. Future work is required. We will investigate the proposed approach in different scenarios of social interaction (i.e., in front of group discussion) and dynamic environments. Additionally, various types of intelligent control should be considered to enhance the decision making for autonomous system.

Furthermore, it is raised a promising research issue that the constrained parameter set could be optimized by using machine learning techniques.

Note to practitioners. In general, the robot trajectory is scheduled and planned in host computer and human could wear the tracking device to avoid collision. However, in some emergent cases, robot must be clearly aware the human appearance and actively prevent collision. Thus, the proposed method achieves the purpose of collision avoidance and socially interactive action. Additionally, the switching mechanism to decide proper strategy based on the distancing communication between human and robot is suggested in this work. It is potentially utilized in logistic warehouse, service restaurant, and so on.

Data Availability

No data were used to support this study.

Conflicts of Interest

The authors declare that they have no conflicts of interest.

Acknowledgments

The authors acknowledge the support of time and facilities from Ho Chi Minh City University of Technology (HCMUT), VNU-HCM, for this study.

References

[1] W. Shi, H. Kuang, L.-Y. Dong, and S.-Q. Dai, "Characteristics of lane changing induced by bus stop and deceleration area," in *Proceedings of the Fourth International Joint Conference on Computational Sciences and Optimization*, pp. 1064–1068, Yunnan, China, April 2011.

[2] Y. Wu, J. Xie, L. Duand, and Z. Hou, "Analysis on traffic safety distance of considering the deceleration of the current vehicle," in *Proceedings of the Second International Conference on Intelligent Computation Technology and Automation*, pp. 491–494, Hunan, China, June 2009.

[3] T. Yamamoto, M. Nakamura, and A. U. T. Toriyama, "A study of deceleration behavior for cognitive dysfunction drivers on public road," in *Proceedings of the International Conference on Intelligent Informatics and Biomedical Sciences*, pp. 376-377, Okinawa, Japan, 2015.

[4] Y. Ying and Z. Yuhui, "Virtual simulation experiment analysis of Chevron deceleration marking based on driving simulator," in *Proceedings of the Fourth International Conference on Intelligent Computation Technology and Automation*, pp. 991–994, Guangdong, China, 2011.

[5] T. Wada, S. Doi, N. Tsuru, K. Isaji, and H. Kaneko, "Formulation of deceleration behavior of an expert driver for automatic braking system," in *Proceedings of the International Conference on Control, Automation and Systems*, pp. 2908–2912, Seoul, Republic of Korea, 2008.

[6] C. Miyajima, H. Ukai, A. Naito, H. Amata, N. Kitaoka, and K. Takeda, "Driver risk evaluation based on acceleration, deceleration, and steering behavior," in *Proceedings of the IEEE International Conference on Acoustics, Speech and Signal Processing*, pp. 1829–1832, Prague, Czech Republic, 2011.

[7] D. Ji, B. Wu, C.-W. Min, Z. Guo, Z. Xiao, and F.-H. He, "Deceleration control by the coning motion for CAV terminal guidance without velocity profile," in *Proceedings of the 35th Chinese Control Conference*, pp. 5747–5751, Chengdu, China, 2016.

[8] Z. Jianyong and L. Yuechao, "Simulation on pneumatic brake control of train based on deceleration feedback," in *Proceedings of the Fourth International Conference on Intelligent Computation Technology and Automation*, pp. 928–931, Shenzhen, China, March 2011.

[9] N. Nikolakis, V. Maratos, and S. Makris, "A cyber physical system (CPS) approach for safe human-robot collaboration in a shared workplace," *Robotics and Computer-Integrated Manufacturing*, vol. 56, pp. 233–243, 2019.

[10] M. Safeea and P. Neto, "Minimum distance calculation using laser scanner and IMUs for safe human-robot interaction," *Robotics and Computer-Integrated Manufacturing*, vol. 58, pp. 33–42, 2019.

[11] H. Liu and L. Wang, "Collision-free human-robot collaboration based on context awareness," *Robotics and Computer-Integrated Manufacturing*, vol. 67, p. 101997.

[12] Y. Tian, G. Wang, L. Li, T. Jin, F. Xi, and G. Yuan, "A universal self-adaption workspace mapping method for human-robot interaction using Kinect sensor data," *IEEE Sensors Journal*, vol. 20, 2020.

[13] C. Zong, Z. Ji, J. Yu, and H. Yu, "An angle-changeable tracked robot with human-robot interaction in unstructured environments," *Assembly Automation*, vol. 40, no. 4, pp. 565–575, 2020.

[14] H. Wang, S. Wang, J. Yao et al., "Effective anti-collision algorithms for RFID robots system," *Assembly Automation*, vol. 40, 2019.

[15] C. Zong, Z. Ji, and H. Yu, "Dynamic stability analysis of a tracked mobile robot based on human–robot interaction," *Assembly Automation*, vol. 40, 2019.

[16] A. M. Zanchettin, P. Rocco, S. Chiappa, and R. Rossi, "Towards an optimal avoidance strategy for collaborative robots," *Robotics and Computer-Integrated Manufacturing*, vol. 59, pp. 47–55, 2019.

[17] J. Funke, M. Brown, S. M. Erlien, and J. C. Gerdes, "Collision avoidance and stabilization for autonomous vehicles in emergency scenarios," *IEEE Transactions on Control Systems Technology*, vol. 25, no. 4, pp. 1204–1216, 2016.

[18] X. He, Y. Liu, C. Lv, X. Ji, and Y. Liu, "Emergency steering control of autonomous vehicle for collision avoidance and stabilisation," *Vehicle System Dynamics*, vol. 57, no. 8, pp. 1163–1187, 2019.

[19] X. Huang, W. Wu, H. Qiao, and Y. Ji, "Brain-inspired motion learning in recurrent neural network with emotion modulation," *IEEE Transactions on Cognitive and Developmental Systems*, vol. 10, no. 4, pp. 1153–1164, 2018.

[20] S. Guo, L. Feng, Z.-B. Feng et al., "Multi-view laplacian least squares for human emotion recognition," *Neurocomputing*, vol. 370, pp. 78–87, 2019.

[21] E. Zheng, J. Wan, L. Yang, Q. Wang, and H. Qiao, "Wrist angle estimation with a musculoskeletal model driven by electrical impedance tomography signals," *IEEE Robotics and Automation Letters*, vol. 6, no. 2, pp. 2186–2193, 2021.

[22] H. Su, A. Mariani, S. E. Ovur, A. Menciassi, G. Ferrigno, and E. De Momi, "Toward teaching by demonstration for robot-assisted minimally invasive surgery," *IEEE Transactions on Automation Science and Engineering*, vol. 18, no. 2, pp. 484–494, 2021.

[23] H. Su, C. Yang, G. Ferrigno, and E. De Momi, "Improved human-robot collaborative control of redundant robot for t minimally invasive surgery," *IEEE Robotics and Automation Letters*, vol. 4, no. 2, pp. 1447–1453, 2019.

[24] H. Su, W. Qi, Y. Hu, H. R. Karimi, G. Ferrigno, and E. De Momi, "An incremental learning framework for human-like redundancy optimization of anthropomorphic manipulators," *IEEE Transactions on Industrial Informatics*, vol. 18, no. 3, pp. 1864–1872, 2020.

[25] Q. Yang, D. Qu, F. Xu, F. Zou, G. He, and M. Sun, "Mobile robot motion control and autonomous navigation in GPS-denied outdoor environments using 3D laser scanning," *Assembly Automation*, vol. 39, 2019.

[26] D. Sanders, "Comparing speed to complete progressively more difficult mobile robot paths between human tele-operators and humans with sensor-systems to assist," *Assembly Automation*, vol. 29, 2009.

[27] D. Chen, Q. Lu, D. Peng, K. Yin, C. Zhong, and T. Shi, "Receding horizon control of mobile robots for locating unknown wireless sensor networks," *Assembly Automation*, vol. 39, 2018.

[28] J. Luo, D. Huang, Y. Li, and C. Yang, "Trajectory online adaption based on human motion prediction for teleoperation," *IEEE Transactions on Automation Science and Engineering*, 2021.

[29] J. Luo, Z. Lin, Y. Li, and C. Yang, "A teleoperation framework for mobile robots based on shared control," *IEEE Robotics and Automation Letters*, vol. 5, no. 2, pp. 377–384, 2019.

[30] C. Morato, K. N. Kaipa, B. Zhao, and S. K. Gupta, "Toward safe human robot collaboration by using multiple kinects based real-time human tracking," *Journal of Computing and Information Science in Engineering*, vol. 14, no. 1, 2014.

[31] A. Mohammed, B. Schmidt, and L. Wang, "Active collision avoidance for human-robot collaboration driven by vision sensors," *International Journal of Computer Integrated Manufacturing*, vol. 30, no. 9, pp. 970–980, 2017.

[32] S. Kumar, D. Gupta, and S. Yadav, "Sensor fusion of laser & stereo vision camera for depth estimation and obstacle avoidance," *International Journal of Computer Application*, vol. 1, no. 26, pp. 22–27, 2010.

[33] P. A. Lasota, G. F. Rossano, and J. A. Shah, "Toward Safe Close-Proximity Human-Robot Interaction with Standard Industrial Robots," in *Proceedings of the IEEE International Conference on Automation Science and Engineering (CASE)*, pp. 339–344, Taipei, Taiwan, August 2014.

[34] M. Galvani, F. Biral, B. M. Nguyen, and H. Fujimoto, "Four wheel optimal autonomous steering for improving safety in emergency collision avoidance manoeuvres," in *Proceedings of the IEEE 13th International Workshop on Advanced Motion Control (AMC)*, pp. 362–367, IEEE, Yokohama, Japan, March 2014.

[35] H. Q. T. Ngo, V. N. Le, V. D. N. Thien, T. P. Nguyen, and H. Nguyen, "Develop the socially human-aware navigation system using dynamic window approach and optimize cost function for autonomous medical robot," *Advances in Mechanical Engineering*, vol. 12, no. 12, 2020.

[36] K. H. Rew and K. S. Kim, "A closed-form solution to asymmetric motion profile allowing acceleration manipulation," *IEEE Transactions on Industrial Electronics*, vol. 57, no. 7, pp. 2499–2506, 2010.

[37] X.-T. Truong and T.-D. Ngo, ""To approach humans?": a unified framework for approaching pose prediction and socially aware robot navigation," *IEEE Transactions on Cognitive and Developmental Systems*, vol. 10, no. 3, pp. 557–572, 2018.